Analyzing The Throughput of Online Home Users During the COVID-19 Pandemic Using the Neyman-Scott Cluster Process

Abdel Karim Ajami, Hassan Artail

Electrical and Computer Engineering Department
American University of Beirut (AUB)
Beirut, Lebanon 30332–0250
E-mails: {aa377, hartail}@aub.edu.lb

***Abstract*—With the recent outbreak of the COVID-19 pandemic, major industries and academic institutions throughout the world have moved into a work-from-home situation, which resulted in a huge demand for networking resources. In particular, several home users are demanding simultaneously high data rates to support online video streaming applications, like Webex and Zoom. Therefore, it is expected that in these situations the quality of experience of online users may be severely affected or deteriorated, especially as the number of simultaneous active online users increases. In this paper, we use the Neyman-Scott Cluster Process from Stochastic Geometry to model the spatial patterns of online home users and analyze the throughput that could be achieved by a various numbers of online home users who are accessing the internet concurrently.**

***Index Terms*—Home Users; Stochastic Geometry; Neyman-Scott Cluster Process; Area System Throughput;**

I. Introduction and Related Work

Since December 2019, the Coronavirus disease 2019 or COVID-19 has spread like wildfire throughout the world, thus forcing major industries and institutions of all types to moved to a work-from-home mode where employees, faculty, and students have started working from home using mobile computing devices to deliver their job duties. This led to an increase in the number of simultaneous home users who use video streaming applications, most notably Webex, Zoom, and Microsoft's Groups applications [1]. In the literature, researchers have worked on several research topics related to COVID-19. For example, in [2], the authors used existing cellular wireless network functionalities to detect regions at risk for spreading COVID-19. On the other hand, in [3], the authors presented a headset like wearable device to track COVID-19 symptoms. Whereas in [4], the authors discuss the impact of COVID-19 pandemic on teaching and present an online teaching model based on the idea of Problem-Based Learning (PBL) and take "Data Structure" as an example to discuss the design of teaching process and problems. But to the best of our knowledge, there is no work so far that have analyzed the impact of the pandemic on the capacity of Wi-Fi networks. Especially in home networks where the users connect to Wi-Fi hotspots usually with closed access (encrypted communications). Thus, it is worth to investigate the case when these Wi-Fi hotspots are heavily loaded during pandemics and analyze the impact of this load on the throughput of simultaneous online home users.

The network and software community recognized early on the crucial role that computer networks play in the functioning of distributed and Internet applications. It responded to the need of ensuring their reliable and efficient operations by developing and proposing different methods and approaches for testing network systems and servers. A series of patents started to appear as of early 2000 on the subject of network, server, an protocol testing. Starting with [5], a method and system were developed for simulating multiple concurrent clients on a network server to stress test the server. The method in [6] is similar, although it is a software-based tool that aims to test network servers under high load scenarios. In [7] and [8], a method of testing a cellular network was proposed and involved creating network traffic using a mobile phone that is connected to a computer. The computer measures the response to the test traffic and the functioning of the network. In [9], a set of methods and media were created for stress testing mobile network equipment by simulating multiple user equipment devices. Generated messages were transmitted over a common public radio interface to a radio equipment controller to stress test it. Finally, the patent in [10] describes a network testing method that is implemented in a software-defined network (SDN), where testing is accomplished by injecting network events using an SDN controller, and gathering network traffic statistics. In addition to patents, several works appeared in the literatures on network performance testing. In [11], the authors proposed a method and set of tools for test case generation that is meant to stress test multimedia systems. It adapts constraint solving techniques to generate test cases that lead to potential resource saturation in such systems. A stress test methodology was proposed in [12] that is aimed at increasing the chances of discovering faults related to network traffic in distributed systems. The technique analyzes control flow in sequence diagrams, and produces stress test requirements that are made of specific control flow paths along with timing

978-1-6654-2854-5/21/$31.00 ©2021 IEEE

information indicating when to trigger them. Finally, motivated by the need to do proactive network testing, the work in [13] is based on the notion of gathering information on normal network operations in order to have a base to compare with when problems occur.

In contrast to the above methods, tools, and approaches, our technique in this paper uses Stochastic geometry which is a popular tool to analyze wireless networks [16]–[19]. Due to the inhomogeneities in city's building formation, the density of Wi-Fi access points (APs) (or hotspots) cannot be treated uniformly, where in some places the density of APs is higher, whereas in other places it decrease to zero. In such cases, the homogeneous 2D Poisson Point Process (PPP) may not offer accurate results [20]. An efficient alternative is the Cluster based model such as the Poisson Cluster Process (PCP) that provides tractable and accurate analytical model for home Wi-Fi networks [21]. The aim of this paper is to analyze the user throughput of heavily loaded home Wi-Fi networks resulting from an increased number of simultaneous home users that demand high data rates using the Neyman-Scott Cluster process, a member of the family of Poisson Cluster processes.

The rest of the paper is organized as follows. The system model including a description of the Neyman-Scott Cluster process is given in section II. Section III provides the computation of the area system throughput (AST). The performance analysis is provided in Section IV and finally Section V concludes the paper.

II. System Model

We consider a network of Wi-Fi APs and users. The locations of the Wi-Fi APs are distributed according to a Neyman-Scott cluster point process ϕ [14], [15]. The Neyman-Scott cluster point process is a Poisson cluster process that consists of a parent process forming the center of the clusters and the daughter points that are spatially distributed around the cluster centers. The parent points are distributed on the plane according to a homogeneous Poisson point process (PPP) with intensity λ_p. Note that the parent points themselves are not physically included but only denote the center of the clusters. The daughter points of the representative cluster are scattered independently and with identical distribution around the center of each cluster. For the daughter process we consider the Matérn cluster process where the number of daughter points follows a Poisson distributed with mean $\hat{c}$ and each daughter point is uniformly distributed in a radius R around the origin with density function $f(\mathbf{x})$ given by:

$$f(\mathbf{x}) = \begin{cases} \frac{1}{\pi R^2} & \text{if } ||\mathbf{x}|| \leq R \\ 0 & \text{otherwise} \end{cases} \quad (1)$$

where x is the two dimensional coordinates relative to the cluster center, and $||.||$ is the Euclidean norm. In this model, the daughter points represent the Wi-Fi APs as shown in Figures 1 and 3. The density of ϕ is defined as λ which is composed of the parent process with density λ_p and the average number of daughter points $\hat{c}$ within each cluster resulting in $\lambda = \lambda_p \hat{c}$.

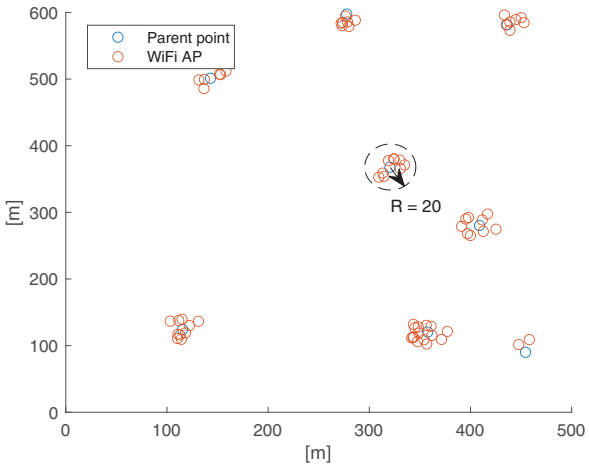

Fig. 1: Matérn Cluster Process (R = 20 m, $\lambda_p = 20/\text{km}^2$, $\hat{c} = 10$)

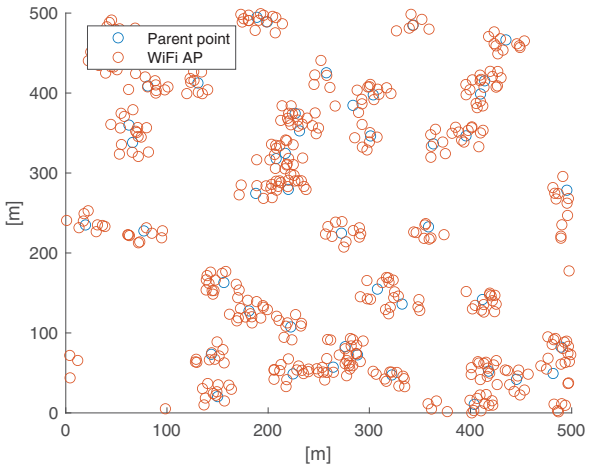

Fig. 2: Matérn Cluster Process (R = 20 m, $\lambda_p = 200/\text{km}^2$, $\hat{c} = 10$)

The receiver is not considered a part of the process. The power received by a receiver located at z due to a transmitter at x is modeled as $h_x g(x - z)$ where h_x is the power fading coefficient associated with the channel between the nodes x and z. We assume that all fading coefficients are independent and identically distributed (i.i.d) Rayleigh distributed with mean $\mu = 1$. The function $g(x - z)$ corresponds to the path loss function where $g(x - z) = ||x - z||^{\alpha}$ where $\alpha \geq 2$ is the path loss exponent. We let o denote the origin $(0, 0)$, and assume the locations of the Wi-Fi users to be subject to a homogeneous PPP with intensity λ_u that is independent of the location of the Wi-Fi APs.

In this paper, we assume that a typical mobile user is located at z and is communicating with a Wi-Fi AP, which is located

at the origin based on Palm measures [14]. The whole point process can be translated such that the mobile user can be considered to be located at the origin. We assume also that the typical user chooses a serving AP based on the maximum average received power, i.e. the minimum distance to the user.

III. Coverage Probability

To characterize the Matérn Cluster process, we use the Probability Generating Functional (PGFL) which is defined for the Matérn Cluster process as follows:

$$G_N\left(v\right)=\exp\left(-\lambda_p\int_{\mathbb{R}^2}\left[1-G_s(v(\mathbf{x}))\right]\mathrm{d}\mathbf{x}\right), \quad (2)$$

where vector $v(\mathbf{x})$ denotes the location of the Wi-Fi APs and $0\leq v(\mathbf{x})\leq 1$ for all $\mathbf{x}\in\mathbb{R}^2$. In addition, $G_s\left(v(\mathbf{x})\right)$ is defined as follows:

$$G_s\left(v(\mathbf{x})\right)=\exp\left(\hat{c}\left[\int_{\mathbb{R}^2}\left[v(\mathbf{x}+\mathbf{y})f(\mathbf{x})d\mathbf{y}-1\right]\right]\right), \quad (3)$$

with $f(\mathbf{x})$ defined in (1).

The coverage probability is defined as the probability that the SINR is higher (or at least equal), than a predefined threshold value (T), which is defined as a specific system parameter. The SINR coverage probability of a Wi-Fi user at a distance $||z||$ from the Wi-Fi AP which is located at the origin can be derived by using the PGFL in (3) as follows:

$$\mathbb{P}_c\left(\mathbf{z},T\right)=\exp\left(-\lambda_p\int_{\mathbb{R}^2}\left[1-\exp\left(-\hat{c}\,\beta(\mathbf{z},\mathbf{x},T)\right)\mathrm{d}\mathbf{x}\right]\right)\times\int_{\mathbb{R}^2}\exp\left(-\hat{c}\,\beta(\mathbf{z},\mathbf{y},T)\right)f(\mathbf{y})\mathrm{d}\mathbf{y}, \quad (4)$$

where

$$\beta(\mathbf{z},\mathbf{x},T)=\int_{\mathbb{R}^2}\frac{g\left(\mathbf{x}-\mathbf{y}-\mathbf{z}\right)}{\frac{g(\mathbf{z})}{T}+g\left(\mathbf{x}-\mathbf{y}-\mathbf{z}\right)}f(\mathbf{y})\mathrm{d}\mathbf{y}, \quad (5)$$

where the vectors $\mathbf{x}$ and $\mathbf{y}$ denote the locations of the parent and daughter points (for the particular parent), respectively.

A. Average Coverage Probability

The average coverage probability is computed by considering the coverage probability inside and outside the cluster. When the typical user is located inside the cluster of Wi-Fi APs, the average coverage probability is defined as:

$$\mathbb{P}_{c,in}\left(T\right)=\int_0^{2R}\mathbb{P}_c\left(\mathbf{z},T\right)f_{D_{in}}\left(\mathbf{z}\right)\mathrm{d}\mathbf{z}, \quad (6)$$

where

$$f_{D_{in}}\left(\mathbf{z}\right)\approx\frac{2\bar{c}}{R^2\left(1-\exp\left(-4\bar{c}\right)\right)}\mathbf{z}\exp\left(\frac{-\bar{c}\mathbf{z}^2}{R^2}\right). \quad (7)$$

On the other hand, when the typical user is located outside the cluster of Wi-Fi APs, the average coverage probability is defined as:

$$\mathbb{P}_{c,out}\left(T\right)=\int_0^{\infty}\mathbb{P}_c\left(\mathbf{z},T\right)f_{D_{out}}\left(\mathbf{z}\right)\mathrm{d}\mathbf{z}, \quad (8)$$

where

$$f_{D_{out}}\left(\mathbf{z}\right)=2\pi\lambda_p(\mathbf{z}+R)\exp\left[-\pi\lambda_p(\mathbf{z}^2+2R\mathbf{z})\right]. \quad (9)$$

Thus, the total average coverage probability of a Wi-Fi user at a distance $||z||$ from the Wi-Fi AP is defined as:

$$\mathbb{P}_{c,tot}\left(T\right)=\mathbb{P}_{c,in}\left(T\right)\cdot P(z\,\text{inside Cluster}) \quad (10)$$

$$+\,\mathbb{P}_{c,out}\left(T\right)\cdot P(z\,\text{outside Cluster}), \quad (11)$$

where $P(z\,\text{inside Cluster})$ denotes the probablity that the user is inside the cluster of Wi-Fi APs and is defined as:

$$P(z\,\text{inside Cluster})=1-\exp\left(-\pi\lambda_{\mathrm{p}}\mathrm{R}^2\right). \quad (12)$$

Whereas $P(z\,\text{outside Cluster})$ denotes the probablity that the user is outside the cluster of Wi-Fi APs and is defined as:

$$P(z\,\text{outside Cluster})=\exp\left(-\pi\lambda_{\mathrm{p}}\mathrm{R}^2\right) \quad (13)$$

IV. Area System Throughput (AST)

The area system throughput (AST) of a Wi-Fi AP is defined as:

$$\mathrm{AST}\left(\lambda_{\mathrm{p}},\hat{\mathrm{c}}\right)=\lambda_p\,\hat{c}\,\mathbb{P}_M(\lambda_p,\hat{c})\,BW\int_0^{\infty}\mathbb{P}_{c,tot}(2^x-1)\mathrm{d}x. \quad (14)$$

Where BW corresponds to the frequency bandwidth and $\mathbb{P}_M(\lambda_p,\hat{c})$ corresponds to the medium access probability; the probability that a Wi-Fi AP has access to the channel when it has data to transmit. $\mathbb{P}_M$ accounts for the expected fraction of time that the transmitting Wi-Fi AP has access to the channel, and hence it is a measure of the expected fraction of active transmitters, over a fully overlapped coverage area. For a Wi-Fi AP $\zeta_j\in\Phi$, $\mathbb{P}_M$ can be derived first by using the medium access indicator $\hat{e}_j$ as follows:

$$\hat{e}_j=\prod_{\zeta_i\in\Phi\setminus\{\zeta_j\}}\left(\mathbb{1}_{t_i\geq t_j}+\mathbb{1}_{t_j<t_i}\mathbb{1}_{G_{ij}/l(\|\zeta_i-\zeta_j\|)\leq\Gamma_{cs}/P_w}\right) \quad (15)$$

Where $\mathbb{1}_\gamma$ is the indicator function of the event γ, which is equal to one if γ exists and zero otherwise. Γ_{cs} denotes the carrier sensing threshold of the Wi-Fi AP whereas P_w is the Wi-Fi AP transmission power. In addition, $G_{i,j}$ represents the channel fading random variable between Wi-Fi APs ζ_i and ζ_j, respectively. t_i represents the random back-off used by the Wi-Fi AP during the clear channel assessment procedure. t_i is a uniformly distributed random variable in the interval [0, Δ].

Given that a Wi-Fi AP ζ_i has a random back-off timer $t\in[0,\Delta]$ with cumulative distribution function (CDF) $F(t)=\frac{t}{\Delta}$ $\forall\, t\in[0,\Delta]$, the medium access probability $\mathbb{P}_M(\lambda_p,\hat{c})$ is defined as:

$$P_M(\lambda_p,\hat{c})=\frac{1}{\Delta}\int_0^{\infty}\int_0^{\Delta}\exp\big[-\frac{t}{\Delta}\lambda_p\hat{c}N(\zeta_i,\Gamma_{cs},r_0)\big]f_{\|\zeta_i\|}(r)\mathrm{d}t\mathrm{d}r_0. \quad (16)$$

Where

$$N(\zeta_i,r,\Gamma_{cs})=\int_{\mathbb{R}^2\setminus B(o,r)}\exp\left(-\mu\frac{\Gamma_{cs}}{P_w}g(\zeta-\zeta_i)\right)\mathrm{d}\zeta, \quad (17)$$

and

$$f_{\|\zeta_i\|}(r) = 2\pi\lambda_p\hat{c}\, r \exp\left(-\pi\lambda_p\hat{c}r^2\right). \quad (18)$$

The proof of $P_M(\lambda_p, \hat{c})$ in (16) is shown in Appendix A.

V. Performance Evaluation

In this section, we analyze the performance of the clustered Wi-Fi network using different performance metrics. We assume a Wi-Fi AP transmitting power of $P_w = 23$ dBm and carrier sensing threshold $\Gamma_{cs} = -82$ dBm. Also, we assume that the path loss exponent $\alpha = 4$ and we neglect noise for simplicity. In addition, we consider for demonstration a minimum decoding SINR requirement $T_{min} = -2.6$ for a QPSK modulation with a coding rate of 1/8 according to [24]. First, we start by presenting the numerical results of the SINR coverage probability versus the distance $||z||$ between the Wi-Fi AP and the corresponding user with ($\lambda_p = 200/\text{km}^2$, $\hat{c} = 5$, $R = 20\,\text{m}$) as shown in Figure 2. By inspecting Figure 2, we can see that the SINR coverage probability decreases with the increase of the distance between a Wi-Fi AP and the corresponding user where it reaches zero at around $||z||$ = 80 m.

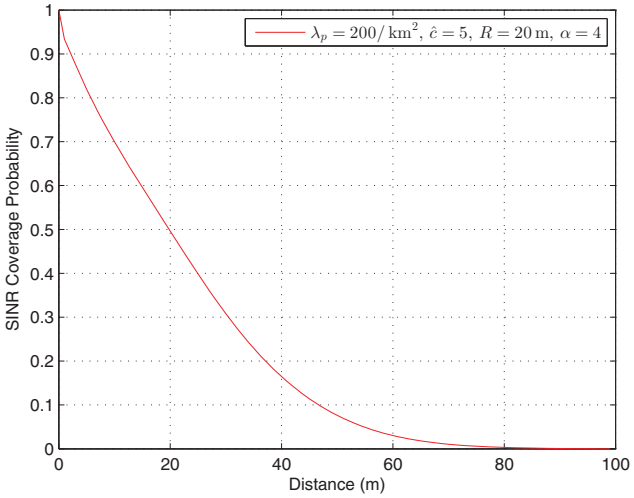

Fig. 3: SINR Coverage Probability versus the distance $||z||$ between Wi-Fi AP and User

Furthermore, we plot the analytical SINR coverage probability versus the variation of λ_p and $\hat{c}$ in Figures 3 and 4, respectively. Figure 3 shows that as the density of parent points λ_p representing the density of clusters increase, the SINR coverage probability decreases from around 0.9 at $\lambda_p = 20/\text{km}^2$ to around 0.1 at $\lambda_p = 700/\text{km}^2$. On the other hand, in Figure 4, we can see that as the average number of Wi-Fi APs $\hat{c}$ increase, the SINR coverage probability decreases from around 0.8 at $\hat{c} = 1$ to around 0.1 at $\hat{c} = 40$. Hence, based on the results provided by Figures 2, 3, and 4, we can see that the increase in the distance between the Wi-Fi AP and the corresponding user as well as the increase in the density of clusters (λ_p) and Wi-Fi APs per cluster ($\hat{c}$) all impact severely the coverage probability and may lead to outage.

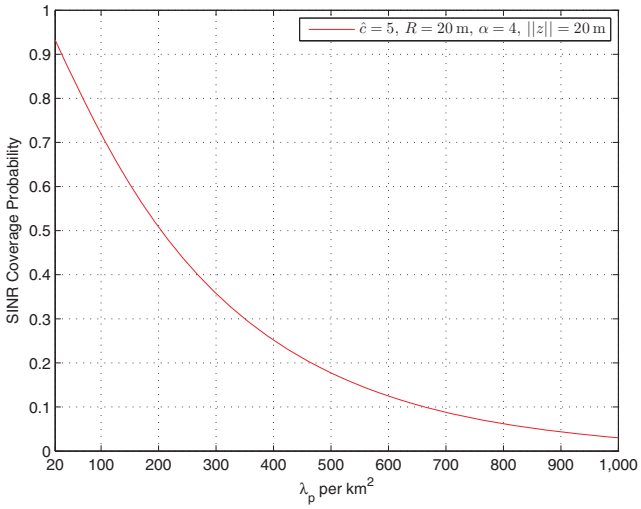

Fig. 4: SINR Coverage Probability versus λ_p

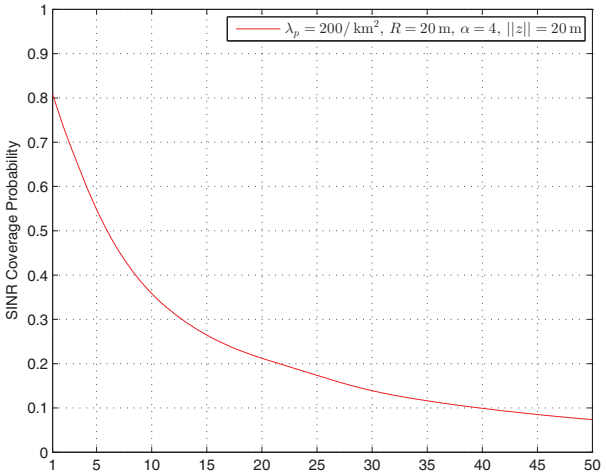

Fig. 5: SINR Coverage Probability versus $\hat{c}$

Next, we present the numerical results for the area system throughput (AST) in Figures 5 and 6. Figure 5 presents the AST of a Wi-Fi network with respect to the variation in the density of clusters λ_p where $\hat{c} = 5$ and $R = 20\,\text{m}$. From Figure 5, we can see that as λ_p increases the AST increases rapidly first in the interval $\lambda_p = [1, 600]$ where it reaches a maximum of 4.3 Gbps at $\lambda_p = 600/\text{km}^2$. Then it starts decreasing as λ_p increases beyond $600/\text{km}^2$ where the AST reaches 1.8 Gbps at $\lambda_p = 3000/\text{km}^2$. Thus, we can see that the throughput could be maximized at $\lambda_p = 600/\text{km}^2$ in the case where $\hat{c} = 5$ and $R = 20\,\text{m}$.

On the other hand, Figure 6 presents the AST of a Wi-Fi network with respect to the variation in the density of Wi-Fi APs per cluster $\hat{c}$ where $\lambda_p = 200/\text{km}^2$ and $R = 20\,\text{m}$. From Figure 5, we can see that as $\hat{c}$ increases the AST increases first in the interval $\hat{c} = [1, 21]$ where it reaches a maximum of 4.7 Gbps at $\hat{c} = 21$. Then it starts decreasing as $\hat{c}$ increases beyond 21 where the AST reaches 2.6 Gbps at $\hat{c} = 50$. Thus,

we can see that the throughput could be maximized at $\hat{c} = 21$ in the case where $\lambda_p = 200/\text{km}^2$ and $R = 20\,\text{m}$.

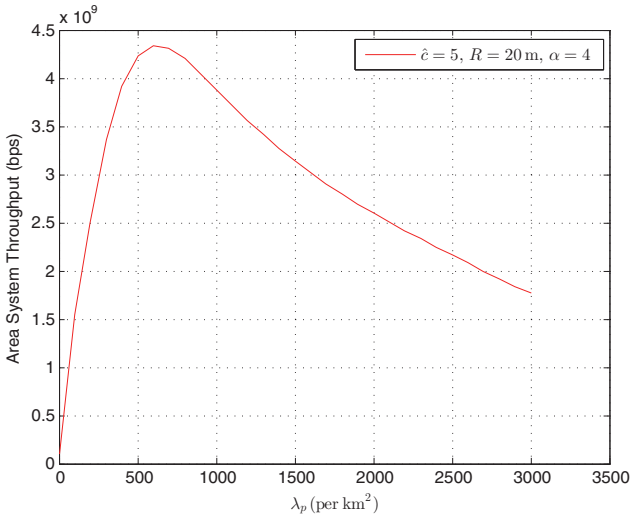

Fig. 6: Area System Throughput (AST) versus λ_p

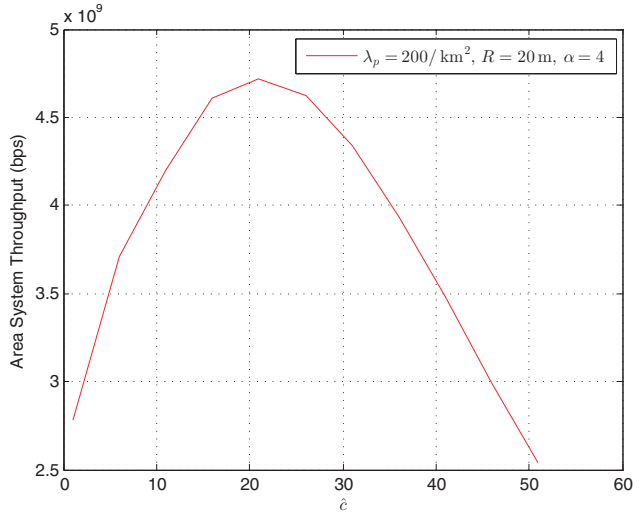

Fig. 7: Area System Throughput (AST) versus $\hat{c}$

VI. Optimization Problem Formulation and Adopted Solution

We investigate the scenario where the operator would like to optimize the performance and has no constraints on the cost. Hence, given the minimum SINR decoding requirement T_{min}, this can be formulated as follows:

$$\begin{aligned} \max \quad & AST(\lambda_p, \hat{c}, T) \\ \text{s.t.} \quad & T \geq T_{min} \end{aligned} \tag{9}$$

Since the function $AST(\lambda_p, \hat{c}, T)$ is nonlinear, we apply the practical and effective global optimization Newton-Raphson technique [22], as shown in Algorithm 1, to find the optimal density of clusters of APs (λ_p) given an average number of APs per cluster $\hat{c}$ and that provide maximum AST performance as in (9).

Algorithm 1. *Finding optimal network density*

require
Initial parent point process density: λ_0
Average daughter points: $\hat{c}$
Cluster radius: R
Maximum number of iterations: N_{Iter}
Define tolerance margin: ϵ
procedure COMPUTE OPTIMAL λ: λ_{opt}
$\lambda_n \leftarrow \lambda_0$
while $(N_{Iter} > 0)$ ***do***

$$f'(\lambda_n) \leftarrow \frac{\partial}{\partial \lambda} AST(\lambda, \hat{c})\Big|_{\lambda=\lambda_n}$$

$$f''(\lambda_n) \leftarrow \frac{\partial^2}{\partial \lambda^2} AST(\lambda, \hat{c})\Big|_{\lambda=\lambda_n}$$

$$\lambda_{n+1} \leftarrow \lambda_n - \frac{f'(\lambda_n)}{f''(\lambda_n)}$$

$$P \leftarrow AST(\lambda, \hat{c})\Big|_{\lambda=\lambda_{n+1}}$$

// To calculate λ_{opt}
if $P \geq (1 - P_{out})$ ***then***
$\lambda_{opt} \leftarrow \lambda_{n+1}$ ***return***
else
$\lambda_n \leftarrow \lambda_{n+1}$
$N_{Iter} \leftarrow N_{Iter} - 1$ ***continue***
end if
end while
end procedure
end

VII. Optimization Results

Here, we utilize the developed optimization framework to compute statistically optimized network topologies that maximize the AST performance of the clustered Wi-Fi network. We consider for demonstration a minimum decoding SINR requirement $T_{min} = -2.6$ dB for a QPSK modulation with a coding rate of 1/8, according to [24]. In addition we consider a cluster radius $R = 20$. Figure 8 presents the optimal density of parent points λ_p representing the density of clusters of Wi-Fi APs versus the average number of APs in each cluster $\hat{c}$. In Figure 8, we can see the optimal λ_p that achieve the highest AST performance for each $\hat{c}$. We start first by $\hat{c} = 5$, where we can see that the optimal AST performance can be achieved at $\lambda_p = 370$ per km^2. Then, we can see that as the average number of APs per cluster $\hat{c}$ increase, the optimal density of clusters of APs decreases exponentially from $\lambda_p = 370$ per km^2 at $\hat{c} = 5$ to $\lambda_p = 85$ per km^2 at $\hat{c} = 20$ and $\lambda_p = 25$ per km^2 at $\hat{c} = 50$.

VIII. Conclusions

This paper presented a framework based on stochastic geometry using the Matern cluster process to analyze the

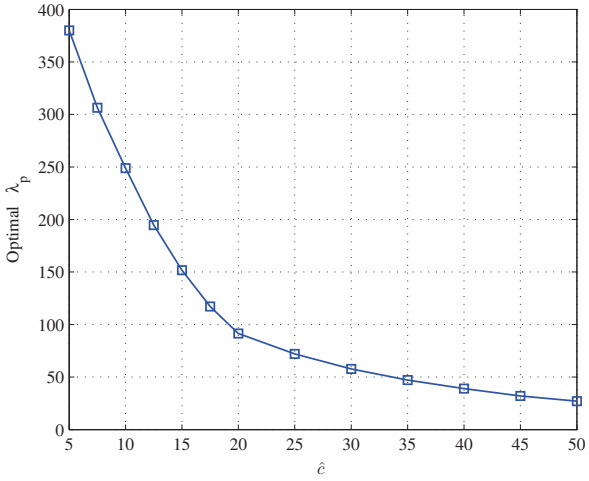

Fig. 8: Optimal λ_p versus $\hat{c}$ using Algorithm 1

throughput of online users during the COVID-19 pandemic. Instead of assuming a fixed medium access probability (MAP) of nodes, we base our model on the IEEE 802.11 standard to derive the MAP of Wi-Fi access points (APs). The model considers the effect of interference as well as the carrier sense multiple access with collision avoidance (CSMA/CA). We then applied the Newton Raphson method to compute the optimal densities of clusters of APs using an average number of APs per cluster, and showed how these optimal densities vary with the density of APs per cluster.

ACKNOWLEDGMENTS

This research was supported by a grant from the American University of Beirut (AUB) University Research Board (URB).

APPENDIX A

Given the tagged Wi-Fi AP $\zeta_j = (r, 0)$, its MAP is derived as:

$$\begin{aligned}
&\mathbb{P}_M(\lambda_p, \hat{c}) = \mathbb{E}\left[\hat{e}_j | t_j = t, \zeta_j = (r_0, 0), \zeta_j \in \Phi\right] \\
&= \mathbb{E}\Bigg[\prod_{\zeta_i \in \Phi \setminus \{\zeta_j\}} \left(\mathbb{1}_{t_i \geq t_j} + \mathbb{1}_{t_j < t_i} \mathbb{1}_{G_{ij}/l(\|\zeta_i - \zeta_j\|) \leq \Gamma_{cs}/P_w}\right)\Bigg] \\
&\overset{(a)}{=} \mathbb{E}\Bigg[\prod_{\zeta_j \in \Phi \cap B^c(0, r_0)} \left(1 - F(t) \exp\left(-\mu \frac{\Gamma_{cs}}{P_w} g\left(\|\zeta_i - \zeta_j\|\right)\right)\right)\Bigg] \\
&\overset{(b)}{=} \exp\Bigg[-F(t)\lambda_p \hat{c} \int_{\mathbb{R}^2 \setminus B(0,r)} \exp\left(-\mu \frac{\Gamma_{cs}}{P_w} g\left(\|\zeta_i - \zeta_j\|\right)\right)\Bigg]
\end{aligned} \tag{3}$$

where (a) follows by re-writing $\zeta_j = (r_0, 0)$ as $\zeta_j \in \Phi$, $\Phi(B^o(0, r_0)) = 0$ and de-conditioning on $\Phi(B^o(0, r_0)) = 0$. By using Slivnyak′s theorem, and the probability generating functional (P.G.FL) of the PPP, (b) is derived. Then by de-conditioning on t with $F(t) = \frac{t}{\Delta}$ and on $||\zeta_j||$ we get the resulting MAP equation in (16).

REFERENCES

[1] Nokia. Redoing the math: the impact of COVID-19 on broadband networks. Accessed: Jun. 11, 2020. Available: https://www.nokia.com/blog/redoing-the-math-the-impact-of-covid-19-on-broadband-networks/

[2] A. A. R. Alsaeedy and E. K. P. Chong,"Detecting Regions At Risk for Spreading COVID-19 Using Existing Cellular Wireless Network Functionalities," in *IEEE Open Journal of Engineering in Medicine and Biology*, vol. 1, pp. 187-189, 2020, doi: 10.1109/OJEMB.2020.3002447.

[3] R. Stojanović, A. Škraba and B. Lutovac, "A Headset Like Wearable Device to Track COVID-19 Symptoms," 2020 9th Mediterranean Conference on Embedded Computing (MECO), Budva, Montenegro, 2020, pp. 1-4, doi: 10.1109/MECO49872.2020.9134211.

[4] Z. Ping, L. Fudong and S. Zheng, "Thinking and Practice of Online Teaching under COVID-19 Epidemic," 2020 IEEE 2nd International Conference on Computer Science and Educational Informatization (CSEI), Xinxiang, China, 2020, pp. 165-167, doi: 10.1109/CSEI50228.2020.9142533.

[5] Michelle M. Rowe,"Server stress testing using multiple concurrent client simulation", US Patent 6,324,492, 2001.

[6] J. Minnis, K. Canady, "Software only tool for testing networks under high-capacity, real-world conditions", US Patent US20060039538A1, 2004.

[7] Y.-F. Ko, R. Dobson, "Network testing systems", US Patent, US7062264B2, 2006

[8] Robert William, Albert Dobson, Yiu Fai Ko, "Network testing and monitoring systems", US Patent US7224968B2, 2007

[9] A. Akman, M. Balkwill, D. Hammond, R. Karp, E. Panofsky, G. Stewart, K. Sundhar, "Methods, systems, and computer readable media for stress testing mobile network equipment using a common public radio interface (CPRI)", US8229416B2, 2012

[10] F. Ivancic, C. Lumezanu, G. Balakrishnan, W. Dennis, A. Gupta, "Network Testing", US Patent US20140337674A1, 2014

[11] J Zhang, SC Cheung, Automated test case generation for the stress testing of multimedia systems, Software: Practice and Experience, 2002 - Wiley Online Library

[12] Vahid Garousi, Lionel C. Briand, Yvan Labiche, "Traffic-aware stress testing of distributed systems based on UML models", In proc. of the 28th international conference on Software engineering, 2006, pp. 391–400.

[13] L. Angrisani, C. Narduzzi, "Testing communication and computer networks: an overview", IEEE Instrumentation & Measurement Magazine, v. 11, n. 5, October 2008.

[14] S. N. Chiu, D. Stoyan, W. S. Kendall, and J. Mecke. Stochastic geometry and its applications. John Wiley & Sons, 2013.

[15] R. K. Ganti and M. Haenggi, "Interference and outage in clustered wireless ad hoc networks," IEEE Trans. Inf. Theory, vol. 55, no. 9, pp. 4067–4086, Sep. 2009.

[16] M. Haenggi. Stochastic geometry for wireless networks. Cambridge University Press, 2012.

[17] H. Q. Nguyen, F. Baccelli and D. Kofman, "A stochastic geometry analysis of dense IEEE 802.11 networks", in *IEEE INFOCOM*, pp. 1199-1207, May 2007.

[18] J. G. Andrews, F. Baccelli, and R. K. Ganti. A tractable approach to coverage and rate in cellular networks. IEEE Transactions on Communications, 59(11):3122–3134, November 2011.

[19] A. k. Ajami and H. Artail, "On The Modeling and Analysis of Uplink and Downlink IEEE 802.11ax Wi-Fi With LTE in Unlicensed Spectrum," *IEEE Trans. Wireless Commun.*, vol. 16, no. 9, pp. 5779-5795, Sept. 2017.

[20] Chou, N.T.; Lin, S.H.; Cheng, S. M.; Chang S.H., "Performance Evaluation of Self-Configured Two-Tier Heterogeneous Cellular Networks," Systems, Man, and Cybernetics (SMC), 2013 IEEE International Conference on, vol. no., pp. 2968-2972, 13-16 Oct. 2013.

[21] Illian, J.; Penttinen, A.; Stoyan, H.; Stoyan, D., "Statistical Analysis and Modelling of Spatial Point Patterns", John Wiley & Sons Publisher ISBN: 978-0-470-02491-2. 2008.

[22] J. H. Mathews, K. K. Fink, "Numerical Methods Using Matlab", Pearson, 4th Edition, 2004.

[23] 3GPP TS 36.213, Technical specification group radio access network; Physical Layer Procedures (Release 14).

[24] S. Sesia, I. Toufik, M. Baker, "LTE the UMTS Long Term Evolution From Theory to Practice", Wiley, 2nd Edition, 2011.